Infrared thermography and ultrasonics to evaluate composite materials for aeronautical applications

S. Boccardi, N.D. Boffa, G.M. Carlomagno, L. Maio, C. Meola[1], F. Ricci

Department of Industrial Engineering - Aerospace Division, University of Naples Federico II, Via Claudio, 21, 80125 Napoli, Italy

[1] Correspondind author: carmeola@unina.it

Abstract. The attention of this paper is focused on the suitability of two techniques: infrared thermography and ultrasonics to evaluate impact damaged carbon/epoxy specimens. The obtained results are compared by highlighting advantages and disadvantages of each technique, as well their limits in view of an integrated use. In this context, a crucial task may be to assess the extension of delamination caused by an impact event, which may ask one to guess between sound and damaged materials at the edge of the instrument background noise. To help fixing this problem, results obtained with either lock-in thermography, or an ultrasonic phased array system, are analysed with the aid of thermographic data collected during impact tests.

1. Introduction

The trend today is towards aircraft completely made of composite materials; the mostly used are Carbon Fiber Reinforced Polymers (CFRPs) [1]. However, they pose some problems mainly linked to their vulnerability to low velocity/energy impact [2] since important damage may arise inside the material thickness without any perception on the impacted side. Then, the availability of non-destructive evaluation techniques (NDE) is of vital importance to ascertain the soundness of a part. Different techniques are today available, but not all are very effective to detect the slim delamination caused by low energy impact.

The attention of the present work is focused on the use of two techniques: phased array ultrasonics (PAUT) and lock-in thermography (LT) to estimate the damage undergone by CFRP specimens under low energy impact. Both techniques are continuously evolving chasing the development of composite materials. In fact, saying composite material means nothing if the type of matrix and fiber is not specified. However, also saying CFRP means nothing since it is sufficient to change the direction of a fiber to have a new material. This, of course, has repercussions on the choice of instrument devices and on setting of test parameters; and then trialing never ends.

Both of the two methodologies are based on well known principles and so no time is spent to dwell in theoretical discourses, but only some basics are recalled which may be helpful to the reader.

PAUT is effective in the detection of most of the common CFRP defects, (such as porosity, slag inclusions and delamination) but has the disadvantage of the needed contact with the part to be inspected. This entails some problems since the surface must be smooth enough to assure good contact, a coupling medium (e.g. oil, ultrasound gel, water, glycerine) is necessary and time is needed to scan large surfaces. In addition, it poses the problem of the custom-built reference blocks which must be fabricated, used and stored following specific rules [3]. LT works without contact and allows

for fast inspection of wide areas, but is affected by loss of contrast in presence of thick parts [4]. Then, an integrated use of LT and PAUT may be advantageous to detect shallow and deep defects saving time in the inspection of large surfaces. However, LT is only an application of infrared thermography (IRT). In fact, IRT, apart from its use as non-destructive evaluation technique, can be also used to take a video during an impact event. It has also been proved that visualization of thermal signatures, caused by local dissipation of impact energy, allows gaining information about the material response to impact [5,6]. In particular, Meola and Carlomagno [5] supplied information on the onset and propagation of impact damage in glass fibers reinforced polymers (GFRP) through the analysis of thermal signatures appearing during an impact event [5] and demonstrated the important role played by manufacturing defects, like porosity and fibers misalignment, in the behavior of GFRP to impact load [6].

In the present work infrared thermography and a phased array system are both used to detect low energy impact damage in carbon fiber reinforced polymers for aeronautical applications. However, rather than discovering for maintenance purposes, impact damage, resulting from the in-service life of a structure, the main interest of the present paper is to ascertain, in a rapid and effective way, the damage caused by an impact of given energy for materials design purposes.

2. Experimental investigation

The used material is a thermoset matrix reinforced with carbon fibers, which is mainly used in the aeronautical field. More specifically, a CFRP panel, 485 by 485 mm with a thickness of 7.8 mm is considered. It includes: Non-Crimp Fabrics (NCF), Multiaxial Reinforcements (MR) and 5 Harness Satin Weave (HSW), being fabricated by the hand lay-up technology and appropriate curing cycle in autoclave. The panel is first non-destructively evaluated with both lock-in thermography (LT) and PAUT, then impacted with a modified Charpy pendulum from one side while an infrared camera views the rear side. The infrared camera takes a sequence of thermal images, which allows monitoring the material thermal behavior under impact. After impact, the specimen is again non-destructively evaluated with both LT and PAUT.

2.1. Monitoring of impact tests

Impact tests are carried out with a modified Charpy pendulum (Figure 1a), which allows enough room for positioning of the infrared camera (Figure 1b) to view the rear specimen surface (i.e., opposite to that struck by the hammer). The test setup is similar to that described in [6], the only difference regards the specimen's lodge which now includes two larger plates with a window 15 cm x 7.5 cm to allow for the contact with the hammer from one side and optical view (by the infrared camera) from the other side. The hammer has hemispherical nose 12.7 mm in diameter. The impact energy E is in the range 50-70 J, chosen to produce only barely visible damage of the panel without perforation and is set by suitably adjusting the falling height of the Charpy arm.

The used infrared camera is the SC6000 (Flir systems), which is equipped with a QWIP detector, working in the 8-9 μm infrared band, NEDT < 35mK, spatial resolution 640x512 pixels full frame, with the pixel size 25 μm x 25 μm, and with a windowing option linked to frequency frame rate and temperature range. Sequences of thermal images are acquired during impact tests at 84 Hz frame rate. To allow for a complete visualization of thermal effects evolution with respect to the ambient temperature, the acquisition starts few seconds before the impact and lasts for some time after. To better analyze the material's thermal behaviour, the first image (t = 0 s) of the sequence, i.e. the specimen surface temperature (ambient) before the impact, is subtracted to each subsequent image so as to generate a map of temperature difference ΔT [5,6]:

$$\Delta T(i,j,t) = T(i,j,t) - T(i,j,0) \quad (1)$$

i and j representing lines and columns of the surface temperature map.

Some ΔT images are shown in figure 2 for varying the impact energy.

a) Charpy pendulum b) specimen lodge and position of the infrared camera

Figure 1. Setup for impact tests

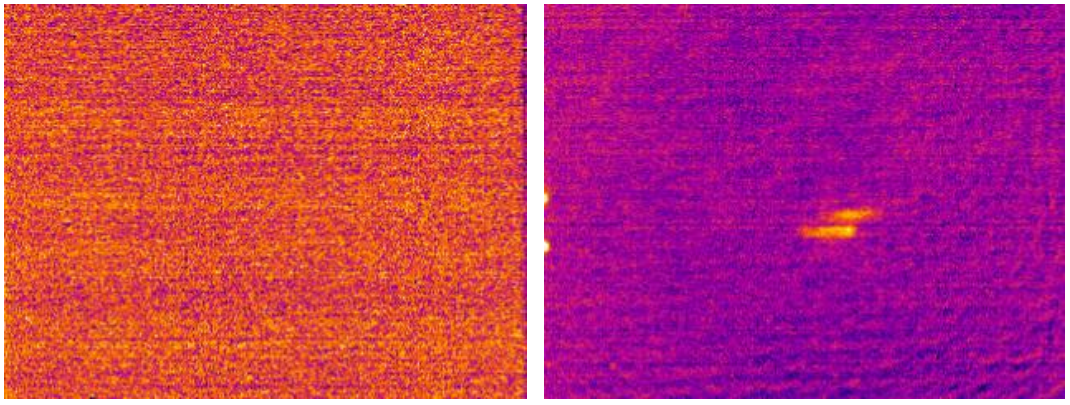

a) Before impact c) 0.024 s after impact at 65 J

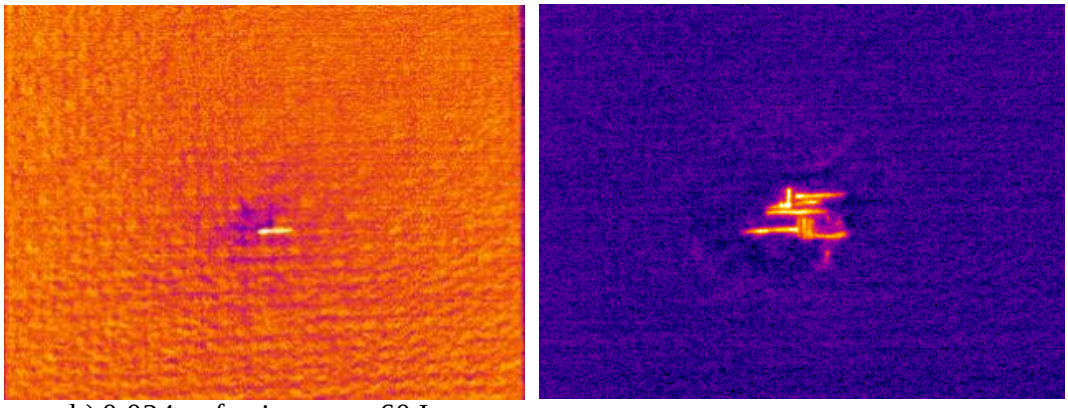

b) 0.024 s after impact at 60 J d) 0.024 s after impact at 70 J

Figure 2. Some ΔT images

More specifically, the first image (Figure 2a) is taken before starting of impact tests, while the other three are taken 0.024 s after impact at 60 J (Figure 2b), 65 J (Figure 2c) and 70 J (Figure 2d). In each image the temperature scale is fine-tuned to highlight any thermal signature induced by the impact; this is the reason why the background colour is not the same, but changes from image to

image. As can be seen, the specimen surface, which is initially (before the impact) at an almost constant ΔT value (almost uniform colour), displays sudden at the impact, temperature variations which strongly depend on the impact energy (Figures 2b-d). In particular, at E = 60 J (Figure 2b) the specimen surface displays a local cooling down, due to thermo-elastic effects, and a short hotter line, accounting for local delamination. By increasing the impact energy to E = 65 J (Figure 2c) two hot lines appear to account for some expansion in delamination. However, the maximum ΔT remains below 0.5 K meaning that no important damage occurred [5,6]. To a further increase of the impact energy to E = 70 J the temperature variations strengthen up and the warm area enlarges (Figure 2d). In particular, owing to also to images not herein shown, thermal signatures display a more complex evolution in time and in space meaning that more important delaminations occurred at different layers through the material thickness. Of course, quantitative data can be obtained by applying ad hoc post-processing procedures to the sequences of thermal images recorded during impact tests.

2.2. Non-destructive evaluation

As already said non-destructive evaluation is performed by using both lock-in thermography and phased array ultrasonic.

2.2.1. Lock-in thermography. The test setup for inspection with lock-in thermography includes the specimen, the infrared camera and two halogen lamps (1 kW each) for harmonic thermal stimulation of the specimen [6]. The infrared camera is the same SC6000 used to monitor the impact, but now is equipped with the IrNDT(R) (AT technology) lock-in option which includes both hardware and software to allow setting up of test parameters, handling of thermal images, visualization and processing of phase (or amplitude) images. Lock-in thermography is a well known technique, so more details can be found elsewhere; herein, only the basic relationship is reported, which links the thermal diffusion length μ to the material average thermal diffusivity α and to the heating frequency f:

$$\mu = \sqrt{\frac{\alpha}{\pi f}} \tag{2}$$

The depth range for the amplitude image is given by μ, while the maximum depth p, which can be reached for the phase image, is equal to 1.8 μ. In general, it is preferable to reduce data in terms of phase image because of its insensitivity to both non uniform heating and local variations of emissivity over the monitored surface. The material thickness, which can be inspected, depends on the wave period (the longer the period, the deeper the penetration) and on the material average thermal diffusivity. According to Eq. 2, the knowledge of the thermal diffusivity is fundamental to evaluate the depth at which any detected anomaly is located, or to choose the frequency value to check the material conditions at a given depth. To this end, the overall thermal diffusivity α is evaluated with the lock-in technique itself, as described in a previous work by Meola et al. [7], and is found to be α = 0.03 cm^2/s.

Figure 3 shows phase images of the whole panel before impact (Figure 3a) and after three impact at 60, 65 and 70 J (Figure 3b). Practically no damage is detected for impact at E = 60 J, while a dark stain may be recognized for E = 65 J, which could be ascribed to the indentation, but the contrast is very poor making difficult any deduction. This bears witness of a relatively reduced sensitivity of lock-in technique because some damage occurred in the panel, evidenced by the warming up of the impact zone (Figure 2). Some damage is clearly visible for the impact performed at E = 70 J. However, by comparing the phase image taken before impact (Figure 3a) to that taken after impact (Figure 3b) it is possible to see unevenness in the matrix and the fibers orientation that masks phase angles variations linked to light impact induced marks.

Some phase images, taken by varying the heating frequency, of the panel zone including the impact at E = 70 J are reported in figure 4. Starting from the impacted highest f value (Figure 4a), it is possible to follow, by decreasing f, the evolution of the damage at the different layers through the thickness as depicted by the white stain. In particular, considering the thermal diffusivity, α = 0.03

cm^2/s, it is also possible to estimate the corresponding depth. Then, for f = 0.88 Hz, the white stain may practically correspond to the surface indentation. Going more in depth, the white stain enlarges and strengthens accounting for some damage there. It is possible to see a two-lobed structure, evolving along the fibres direction, and surrounded by a lighter elliptic-shaped stain, which becomes even more pronounced as f is decreased to 0.36 Hz (p = 3 mm), to 0.26 Hz (p = 3.4 mm). Such a lobed structure tends to merge into a unique structure, which becomes well consolidated for f = 0.12 Hz (p = 5 mm). However, while getting information about the evolution of the damage in depth, with this approach the overall delamination may be underestimated because delamination propagates between fibres and matrix in a rather tortuous way and in a very thin delaminated zone, the variation of the phase angle gets confused with the background. Of course, this problem becomes more important with the increase of the thickness.

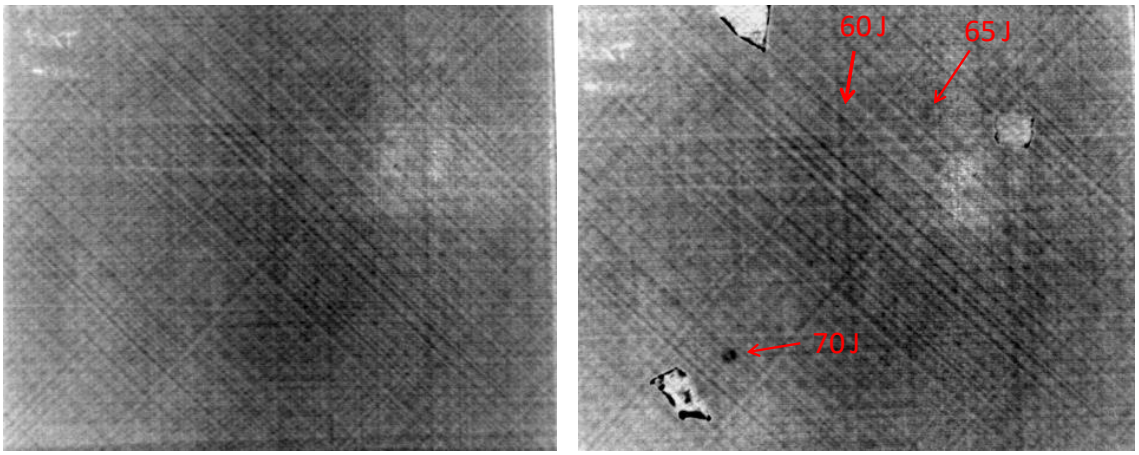

a) before impact b) after three impact at E = 60, 65 and 70 J

Figure 3. Phase images taken at f = 0.15 Hz

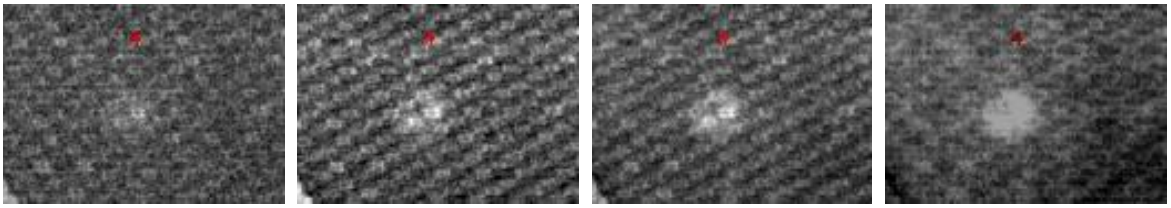

f = 0.88 Hz f = 0.36 Hz f = 0.26 Hz f = 0.12 Hz

Figure 4. Phase images of the area with impact at E = 70 J

2.2.2. Phase array ultrasonic. PAUT is performed with a recently released model by Olympus, the OmniScan SX flaw detector, with a 16:64PR phased array unit, equipped with a conventional UT channel for pulse-echo (PE), pitch-catch or time-of-flight diffraction (TOFD) inspections. Phased array elements are pulsed in such a way to allow multiple beam components to combine with each other and form a single wave front travelling in the desired direction. Similarly, the receiver merges the signals coming from multiple elements into a single representation.

Tests are carried out using an encoded 5 MHz, 64 elements linear array probe with a straight wedge and by using a specific gel as coupling medium. No specific calibration blocks are used, the instrument calibration being obtained by the ultrasonic wave propagation velocity measurement through the test article thickness; it is worth noting that it is difficult to fabricate reference blocks reproducing the CFRP specimen. Tests are carried out with the phased array positioned over the

smooth surface, which coincides with that impacted. The probe is typically moved physically along one axis while the beam electronically scans along the other one, according to the focal law sequence. Signal amplitude or depth data are collected within gated regions of interest and plotted with each focal law progression, using the programmed beam aperture. Data are shown as C-scan images in figure 5. It is possible to see blue-yellow contoured zones in correspondence of the two impacts at 60 and 65 J, which mostly underline an indentation process of the material surface occurred during the impact. However, the indentation damage is too small and below the axial resolution of the B-scan analysis (PAUT limited detection zone, or dead zone). In fact, the time delay between the first interface echo (first surface echo) and the indentation echo is so small that the two impulses are practically superimposed, so it is impossible to detect the imperceptible shallow defect for a correct interpretation. Then, it is possible to infer that not significant damage occurs, but only a faint indentation.

Conversely, more important damage arose under the impact at 70 J. In fact, the articulated and colorful C-scan image bears witness for remarkable damage occurred at the different layers through the thickness. The C-scan amplitude view (Figure 5) shows the presence of a wide intense surface damage; in particular, the central red areolas, indicate significant indentation damage with presence of impact surface penetration and surface cracks. The surrounding yellow/blue areas, with a lower signal amplitude, immediately suggest the presence of more wide delaminations of different orientations and at different depths through the thickness.

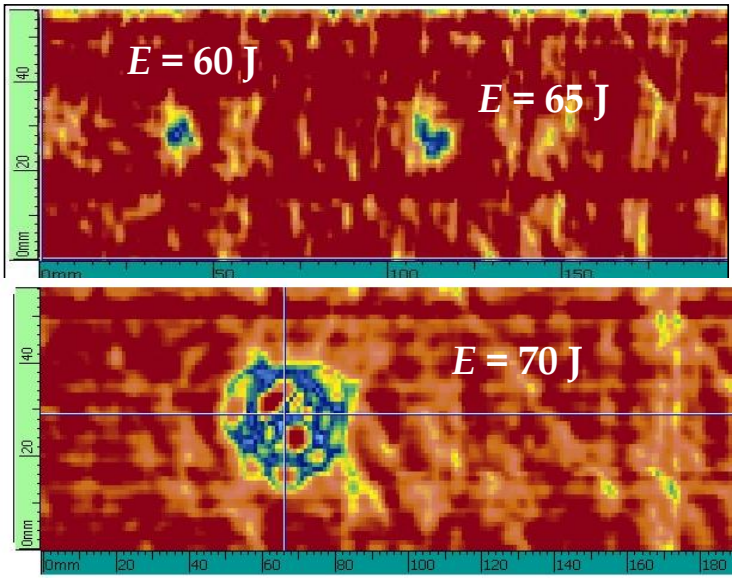

Figure 5. C-scan images

3. Concluding remarks

From a comparison between data coming from LT and PAUT, a general agreement is found. However, to a close view of results obtained for the different impact energies some important comments can be derived. The first observation is that no damage occurs for E = 60 and 65 J, but only surface indentation. In fact, there is a little temperature rise (online monitoring) meaning that the absorbed fraction of the impact energy is very small. On the other side, what PAUT detects is a very superficial discontinuity caused by local indentation. Such a small surface concavity is not detected by LT because the signal gets confused within the noise induced by the material texture. The impact at E = 70 J causes more important damage, which becomes detectable with all the three means: online monitoring, LT and PAUT. A greater fraction of the impact energy is now absorbed which entails a more significant temperature rise, as shown by figure 2d. On the other hand phase images visualize

some damage at the different layers through the thickness (Figure 4). This occurrence is in general validated by the PAUT output (Figure 5) even if a detailed comparison is difficult due to the superposition of all the damaged structures at any depth in the C-scan image. Nevertheless, the two central ovals, which appear (dark-red) in the C-scan image, well match the two-lobed structure which appears in some phase images of figure 4. Also the lenticular structures over the border in the C-scan can be recognised in the phase images. On the whole, with regard to the location in depth of the damage, the PAUT seems more effective since one test is sufficient to supply information about the presence of damage at any depth through the entire thickness. The LT, instead, requires more tests with close variation of the heating frequency, but it is more selective in contouring the damage occurred at a given depth.

References

[1] Soutis C 2005 Fiber reinforced composite in aircraft construction *Progr. Aerosp. Sci.* **41** 143-51.
[2] Richardson M O W and Wisheart M J 1996 Review of low-velocity impact properties of composite materials, *Composites Part A* **27** 1123-31.
[3] Olympus manual: Advances in phased array ultrasonic technology applications.
[4] Meola C and Carlomagno G M 2004 Recent advances in the use of infrared thermography *Meas. Sci. Technol.* **15** R27-R58.
[5] Meola C and Carlomagno G M 2010 Impact damage in GFRP: new insights with Infrared Thermography, *Composites Part A* **41** 1839-47.
[6] Meola C and Carlomagno G M 2014 Infrared thermography to evaluate impact damage in glass/epoxy with manufacturing defects *Int. J Impact Engineering* **67** 1-11.
[7] Meola C, Carlomagno G M, Squillace A and Giorleo G 2002 Non-destructive control of industrial materials by means of lock-in thermography, *Meas. Sci. Technol.* **13** 1583-90.

Acknowledgments

The technical assistance of Mr. G. Sicardi in setting up the experimental apparatus is acknowledged.